THE JOURNAL OF BIOLOGICAL CHEMISTRY VOL. 283, NO. 36, pp. 24738–24747, September 5, 2008

On the Oxygen Reactivity of Flavoprotein Oxidases

*AN OXYGEN ACCESS TUNNEL AND GATE IN BREVIBACTERIUM STEROLICUM CHOLESTEROL OXIDASE**

Received for publication, March 25, 2008, and in revised form, July 2, 2008 Published, JBC Papers in Press, July 9, 2008, DOI 10.1074/jbc.M802321200

Luciano Piubelli[‡], Mattia Pedotti[‡], Gianluca Molla[‡], Susanne Feindler-Boeckh[§], Sandro Ghisla[§], Mirella S. Pilone[‡], and Loredano Pollegioni[‡1]

From the [‡]Department of Biotechnology and Molecular Sciences, University of Insubria, 21100 Varese, Italy and [§]Fachbereich Biologie, University of Konstanz, D-7857 Konstanz, Germany

The flavoprotein cholesterol oxidase from *Brevibacterium sterolicum* (BCO) possesses a narrow channel that links the active center containing the flavin to the outside solvent. This channel has been proposed to serve for the access of dioxygen; it contains at its "bottom" a Glu-Arg pair (Glu-475—Arg-477) that was found by crystallographic studies to exist in two forms named "open" and "closed," which in turn was suggested to constitute a gate functioning in the control of oxygen access. Most mutations of residues that flank the channel have minor effects on the oxygen reactivity. Mutations of Glu-311, however, cause a switch in the basic kinetic mechanism of the reaction of reduced BCO with dioxygen; wild-type BCO and most mutants show a saturation behavior with increasing oxygen concentration, whereas for Glu-311 mutants a linear dependence is found that is assumed to reflect a "simple" second order process. This is taken as support for the assumption that residue Glu-311 finely tunes the Glu-475—Arg-477 pair, forming a gate that functions in modulating the access/reactivity of dioxygen.

Bacterial cholesterol oxidase (CO,[2] EC 1.1.3.6) is a monomeric bifunctional FAD-containing flavoenzyme. It catalyzes the first step in the pathway of cholesterol degradation in a number of soil bacteria (1). From a mechanistic point of view, it catalyzes both the dehydrogenation of the C(3)-OH function of the cholestan system as well as the following isomerization of the intermediate cholest-5-en-3-one to yield cholest-4-en-3-one as the final product (Scheme 1) (2, 3). Redox catalysis by CO can be separated into the two half-reactions, as shown in Scheme 2. The first half-reaction is the reduction of the flavin via hydride transfer from the alcohol (the reductive half-reaction), and the second half-reaction is the oxidation of the reduced flavin by molecular oxygen, the final acceptor (oxidative half-reaction) (4).

CO is a useful biotechnological tool used for the determination of serum cholesterol levels (for review, see Ref. 2); it possesses larvicidal activity (5) and has been developed as an insecticide against *Coeloptera* (5, 6). CO has been discussed as a factor important for infection by the pathogenic bacterium *Rhodococcus equi* (7–9); because this enzymatic activity is unique to bacteria, it represents a potential target for new antibiotics.

From a structural point of view, two different types of CO have been found in nature; COs type I, such as those from *Streptomyces* sp. *SA-COO* and *R. equi* (10) containing non-covalently bound FAD, and type II COs (such as *Brevibacterium sterolicum* CO (BCO), used in this work), in which the cofactor is covalently linked to the protein through an 8-α-N1-histidyl bond to His-121 (corresponding to His-69 in the mature form of BCO) (11). The covalent (type II) and non-covalent (type I) COs differ in many functional properties, such as absorbance spectra, redox potentials (E_m difference ~100 mV), and kinetic mechanisms (sequential *versus* ping-pong mechanism) (12, 13). The three-dimensional structures of both CO types have been solved by Vrielink and coworkers (14, 15); they show completely different tertiary topologies. Type I CO is a member of the glucose-methanol-choline oxidoreductase family (14), whereas the type II CO belongs to the vanillyl-alcohol oxidase subfamily (15), a fold proposed to favor covalent flavinylation.

Despite its basic importance, there are gaps in our knowledge of the mechanism of oxygen activation by flavoproteins and, in particular, by COs as well as its regulation and suppression. COs belonging to both fold classes contain narrow channels extending from the surface to the buried active sites cavity that has been proposed to serve in oxygen access (see Fig. 1 for BCO) (1, 15). In recent years molecular tunnels have emerged as common structural features among different classes of enzymes. In both types of COs the tunnel is flanked mainly by hydrophobic residues (at least in the most external region) and houses a single string of water molecules. This finding suggests that oxygen does not diffuse freely into the active site of COs but that access is modulated by specific, protein-mediated events. Interestingly, both tunnels appear to be gated by an Arg (in BCO, type II CO) or an Asn (in *Streptomyces* sp. *SA-COO*, type I CO) residue, albeit operating in opposite fashions. The tunnel is, thus, closed when the Arg-477 side chain of BCO is positioned at a hydrogen bonding distance of the flavin ring system (compare the alternative positions of Arg-477 side chain reported in Fig. 1). In type I CO the tunnel is open when Asn-485 lies closer

* This work was supported by grants from the Deutsche Forschungsgemeinschaft (to S. G.; GH 2/13) and from Fondo di Ateneo per La Ricerca (to L. Pollegioni, G. M., and L. Piubelli). The costs of publication of this article were defrayed in part by the payment of page charges. This article must therefore be hereby marked "*advertisement*" in accordance with 18 U.S.C. Section 1734 solely to indicate this fact.

[1] To whom correspondence should be addressed: Dept. of Biotechnology and Molecular Sciences, University of Insubria, via J. H. Dunant 3, 21100 Varese, Italy. Tel.: 332-421506; Fax: 0332-421500; E-mail: loredano.pollegioni@uninsubria.it.

[2] The abbreviations used are: CO, cholesterol oxidase; BCO, *B. sterolicum* CO; EMTN, enzyme-monitored turnover.

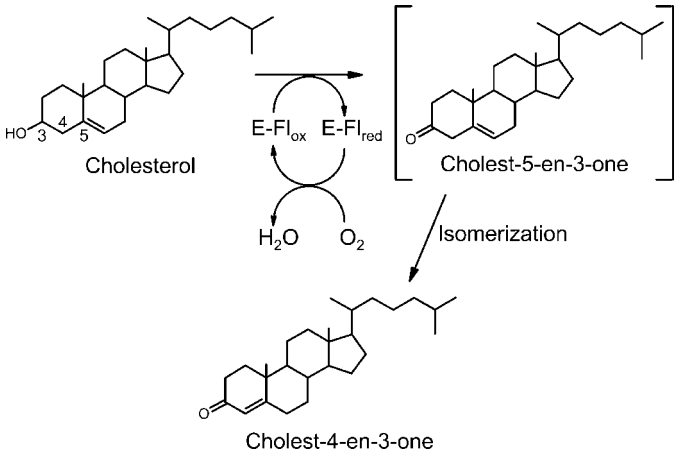

SCHEME 1. **Reaction catalyzed by cholesterol oxidase.**

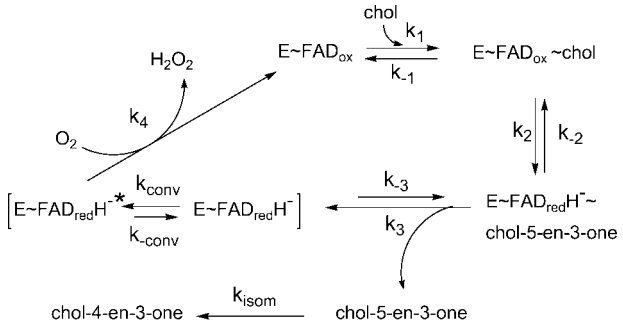

SCHEME 2. **Kinetic mechanism of BCO, adapted from Pollegioni *et al.* (4).** Both the oxidized and reduced forms of BCO are competent in the isomerization reaction (23). k_{conv} and k_{-conv} are steps in which an "interconversion" of species with a different reactivity with dioxygen occurs. k_{isom} stands for the rate of the isomerization reaction depicted in Scheme 1.

to the flavin system (1). These differences might be at the origin of the variance in oxygen reactivity of the two types of COs. In particular, the gating function of the Arg-477 might provide a rationale for the unusual saturation behavior reflected by the kinetics of the reaction of reduced BCO with oxygen (4). We previously proposed that this behavior reflects a reversible conversion of two enzyme forms possessing different oxygen reactivities (*i.e.* E-FAD$^{*}_{red}$ and E-FAD$_{red}$ in Scheme 2); these two species might, thus, correspond to the "open tunnel" and "closed tunnel" conformations identified by the structural analysis (15).

The three-dimensional structure of BCO leads to the identification of several residues other than Arg-477 that could be important for oxygen access/reactivity: Ala-204, Ser-307, Gly-309, Glu-311, Ile-423, and Glu-475 (Fig. 1). The two latter residues in particular adopt two distinct conformations (as Arg-477), and their movements appear to be coordinated with each other and with that of Arg-477 (15).

The scope of the present study is to verify the presence and role of the proposed oxygen tunnel and, in particular, the function of the amino acid side chains possibly forming the mentioned gate. To reach this goal BCO mutants at some of the positions mentioned above were generated and characterized. Comprehension of the mechanism of oxygen reactivity in CO could, thus, shed light on the mechanisms by which flavoprotein oxidases govern the access of and the reactivity with molecular oxygen, this being a fundamental topic in biochemistry that still awaits elucidation. It should be mentioned that similar studies on heme proteins have recently produced important

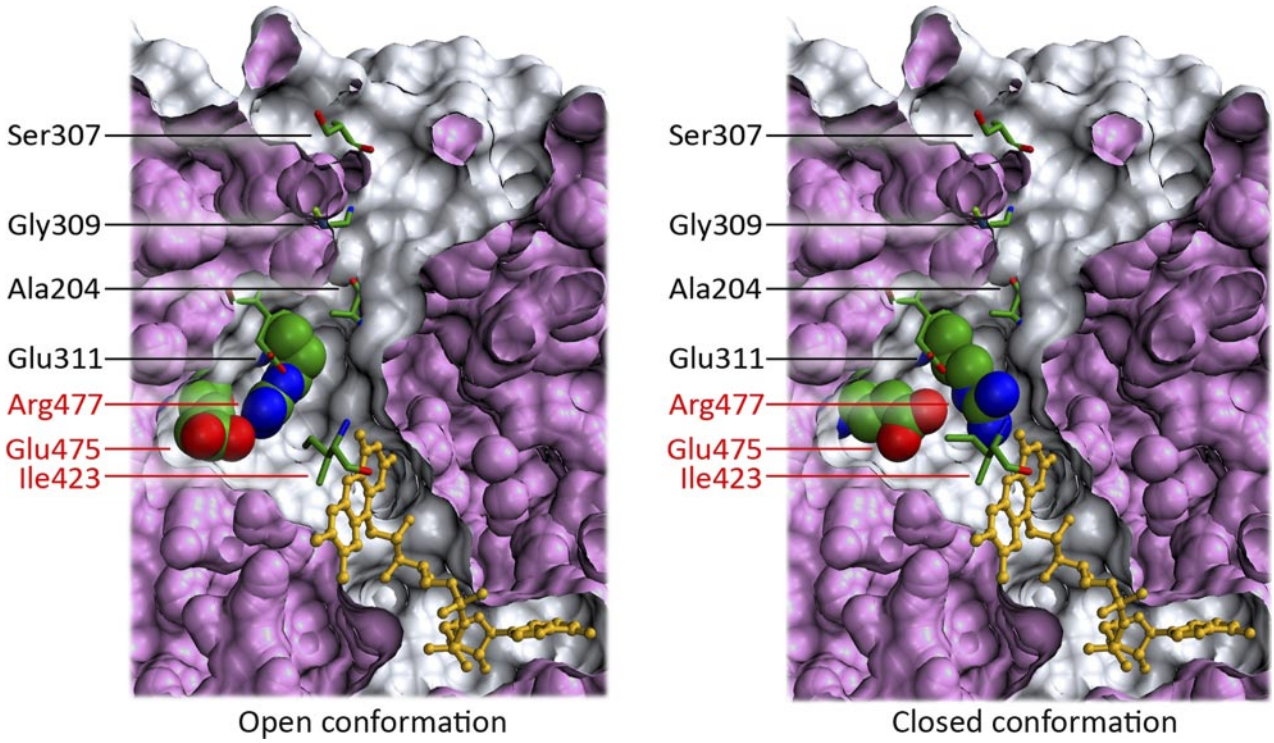

FIGURE 1. **Three-dimensional representation of the assumed oxygen channel of BCO (PDB code 1I19).** The panels depict an open crevice extending from the surface to the active site cavity in which the flavin moiety of the FAD cofactor (*yellow*) is located. In the so-called "open gate" (*left*) and "closed gate" (*right*) conformations the side chains of Ile-423, Glu-475, and Arg-477 adopt different conformations. The latter two are represented with *space-filling models*. Some of the residues shown were subjected to mutagenesis.

insights (16–20) that serve as a guideline and reference for the present study.

EXPERIMENTAL PROCEDURES

Reagents and DNA Manipulation—Restriction enzymes were from New England Biolabs. Enzymatic DNA modifications were carried out according to the manufacturer's instructions and as described in Sambrook *et al.* (21). Plasmid DNA extraction and purification were performed using FlexiPrep™ and Sephaglas™ BandPrep kits from GE Healthcare. Thesit® (polyethylene glycol 400 dodecyl ether), cholesterol, and cholest-5-en-3-one were from Fluka. All chromatographic columns were from GE Healthcare.

Cloning, Mutagenesis, Enzyme Expression, and Purification—A synthetic gene coding for the BCO mature form was obtained from Medigenomix GmbH (Martinsried, Germany). It is based on the amino acid sequence reported in the three-dimensional structure, PDB accession code 1I19 (15). The coding nucleotide sequence was optimized for expression in *Escherichia coli*. The synthetic gene was cloned into the expression plasmid pET24b(+) (Novagen) using NdeI/XhoI restriction sites. Mutagenesis reactions were performed using QuikChange® site-directed mutagenesis kit (Stratagene). Recombinant BL21(DE3)pLysS *E. coli* cells were grown in 2×LB or TB media (Sigma) supplemented with the appropriate antibiotics (chloramphenicol 34 mg/liter and kanamycin 30 mg/liter, final concentration) at 37 °C up to late stationary phase (absorbance at 600 nm, ~1.5–2). Induction was done with isopropyl 1-thio-β-D-galactopyranoside (1 mM final concentration), and cells were collected after 14–26 h of growth at 25 °C. Wild-type and mutant BCOs were expressed in *E. coli* cells in fairly good amounts (about 5 mg of pure enzyme/g cell; 15 mg pure enzyme/liter culture). Recombinant BCOs (all containing a C-terminal His tag) were purified using Ni^{2+} affinity chromatography (HiTrap Chelating HP columns equilibrated with 50 mM potassium phosphate, pH 7.5, 1 M NaCl). Elution of bound enzyme was performed with a linear gradient of imidazole (0–0.5 M) in 50 mM potassium phosphate, pH 7.5, 0.5 M NaCl; recombinant BCOs eluted at about 0.075–0.1 M imidazole. Imidazole was removed by extensive dialysis against 100 mM potassium phosphate buffer, pH 7.5.

Isolation of CO Preparations Devoid of Non-covalently Bound FAD—Recombinant enzyme preparations devoid of non-covalently bound FAD were obtained by exploiting the higher thermolability of the BCO containing non-covalent FAD compared with the covalent form. The substrate cholesterol was also present as the reduced form of BCO containing covalently linked FAD was found to be selectively stabilized. A 1-ml sample of BCO containing 0.5 mM cholesterol was incubated for 3 min at 45 °C. The resulting turbid preparation was centrifuged for 2 min at 12,000 rpm in an Eppendorf tube to yield a clear, yellow supernatant and a white pellet (the non-covalent form of BCO) that was discarded. The supernatant was ultrafiltered through a BIOMAX 5000 membrane (Millipore) to ~10% that of the original volume. This was diluted with 0.1 M potassium phosphate, pH 7.5, and the filtration procedure was repeated. The filtrate contains unmodified FAD, whereas the fraction in the upper chamber consists of BCO containing covalently bound FAD. The ratio of the quantities of FAD present in free form (filtrate) *versus* that bound to BCO (retained fraction) reflects the ratio of non-covalently *versus* covalently FAD-bound BCO forms. The procedure gives BCO preparations with covalently bound FAD at a purity >95% and yields ranging from 20 to 90% that of the starting material, depending on the BCO mutant.

Spectroscopic Experiments—All spectral experiments were carried out at 15 °C in 100 mM potassium phosphate at pH 7.5. Extinction coefficients of the enzyme forms were determined by complete denaturation of the enzyme in 6.4 M guanidinium-HCl, 20 mM potassium phosphate at pH 7.5 assuming that the extinction coefficient of fully denatured enzyme-bound FAD is the same as that of the free FAD (11,300 $M^{-1}\,cm^{-1}$) (22). For the study of the interaction with sulfite, the reagent (sodium salt) was prepared just before use as a 2 M stock solution in 100 mM potassium phosphate, pH 7.5. Aliquots were then added to enzyme (~10 μM), and the changes in absorbance at 450 nm were recorded; this reflects formation of the *N*(5)-sulfite adduct (12). The rate of complex dissociation (k_{off}) was determined spectrophotometrically by following the decay of the complex in a sample that was freed of excess sulfite by gel filtration on a Sephadex G25 column (PD10 column) (12).

Enzymatic Activity and Kinetic Measurements—Kinetic experiments were performed at 25 °C and pH 7.5 in 100 mM potassium phosphate in the presence of 1% Thesit and 1% propan-2-ol (dehydrogenation reaction) or 10% propan-2-ol (isomerization reaction) (v/v final concentrations). Steady-state kinetic measurements at constant O_2 concentration (0.25 mM, air saturation at 25 °C) were performed by monitoring H_2O_2 production using the horseradish peroxidase assay (4 μg/ml, 0.3 mg/ml *o*-dianisidine, $\Delta\epsilon_{440}$ = 13 $mM^{-1}\,cm^{-1}$) as previously described (4, 12, 13). The isomerization reaction (Scheme 1) was followed spectrophotometrically at 240 nm ($\Delta\epsilon_{240}$ = 15.5 $mM^{-1}\,cm^{-1}$). Rapid kinetic measurements were performed as described previously (4, 23) using a BioLogic SFM-300 stopped-flow instrument equipped with a 1-cm path length and interfaced to a J&M diode-array detector. The steady-state kinetics for the reactions at saturating O_2 and cholesterol concentrations was assessed based on the enzyme-monitored turnover (EMTN) method of Gibson *et al.* (24) in which the enzyme was mixed with an equal volume of substrate solution (either aerobic or anaerobic to yield a final O_2 concentration = 0.125 mM) in the stopped-flow instrument. The trace at 446–453 nm (depending on the enzyme form) detects the conversion of oxidized into reduced enzyme forms. For EMTN experiments traces were analyzed according to Gibson *et al.* (24) and using KaleidaGraph™ (Synergy Software). The kinetic traces are treated as records of the rate of catalysis as a continuous function of oxygen concentration. For details about anaerobiosis of enzyme (10–12 μM) and substrate (in the 0.05–0.75 mM range) solutions, see Pollegioni *et al.* (4) and Lim *et al.* (23). For the investigation of the oxidative half-reaction enzymes were reduced with a 3-fold excess of cholesterol under anaerobic conditions and then reacted with buffer solutions equilibrated with different N_2/O_2 mixtures (4). Rapid reactions were routinely monitored by acquiring spectra in the

TABLE 1

Properties of wild-type BCO and mutants upon isolation and purification

The extent of covalently bound FAD present in purified BCO preparations was estimated as described under "Experimental Procedures." The extent of flavin reduction was estimated from the relative decrease of the absorbance at the maximum in the visible region that occurs upon anaerobic addition of cholesterol (2–5 molar excess or as specified in parentheses). The semiquinone form (*R*, red; *B*, blue) was produced by photoreduction. ND, not determined.

Enzyme form	Content of covalent FAD	ϵ/λ_{max}	Flavin reduction by cholesterol		Formation of (red/blue) semiquinone
			Maximal extent	Rate (cholesterol:enzyme ratio)	
	%	$mM^{-1}\ cm^{-1}/nm$	%		% of total
Wild-type					
Commercial[a]	100	13.4/448	100	Fast	$R \sim 70$
Recombinant	40–60	13.4/449	100	Fast	$R \sim 75$
A204C	40–60	11.9/445	100	Fast	ND
G309A	60–70	11.4/447	100	Fast (20:1)	ND
G309C	70–90	12.0/445	100	Fast	ND
E311D	100	11.2/455	100	Fast	$R > 90$
E311Q	100	10.7/458	100	Fast	$R \sim 100$
E311L	100	11.2/453	50	Slow (270:1)	$R \sim 100$
I423L	85	11.8/449	100	Fast (20:1)	ND
I423V	65	11.6/449	100	Fast (20:1)	ND
E475D	100	11.6/455	100	Fast	$R \sim 100$
E475Q	100	12.1/453	100	Fast	$R \sim 100$
R477A	50	12.6/447	50	Extremely slow (300:1)	$B > R$[b]
R477K	60	12.5/448	100	Fast	$R + B \sim 80$

[a] Data are from Gadda *et al.* (12).
[b] Mixture of oxidized and red + blue semiquinone, not quantifiable.

190–700-nm wavelength range with an acquisition time of 0.8 ms/spectrum and resolution of 1 nm (4, 23).

Generation of Reduced Enzyme Forms—The reduction of BCO enzymes was achieved routinely by photoreduction in the presence of EDTA and 5-deaza-riboflavin essentially as described in Gadda *et al.* (12) and Massey and Hemmerich (25) and in 100 mM potassium phosphate buffer, pH 7.5, at 25 °C. Cuvettes with the protein solution were in a water bath at 10–15 °C and at ~15 cm from a 150-W quartz halogen light source. The cuvette was removed at time intervals to record absorption spectra, and this was continued until completion of the process.

Determination of Redox Potentials—For this purpose the xanthine/xanthine oxidase method was employed as reported earlier for wild-type and H69A BCOs (12, 13). The redox indicators used are listed in Table 2.

RESULTS

General Properties of BCO Mutants—Among the BCO variants studied, only mutants at position Glu-311 and Glu-475 were obtained as preparations containing almost exclusively covalently bound FAD (Table 1). Recombinant wild-type BCO as well as most other mutants was obtained as a mixture of enzyme forms containing covalently as well as non-covalently bound FAD (Table 1). The two forms of BCO were identified based on the differences in their absorption spectra (13), and their ratio was estimated as described under "Experimental Procedures." This value is about 1:1 in the case of wild-type and A204C and R477A/K BCO mutants, whereas with G309A/C and I423L/V mutants the covalent form is more prominent (60–80%, Table 1). For these BCO proteins the use of different expression conditions (variation of cultivation media, growth temperatures, and time of recovery after isopropyl 1-thio-β-D-galactopyranoside addition) did not result in the expression of a unique (either covalently or non-covalently bound FAD) protein. The biochemical characterization of all BCO variants was carried out using preparations containing essentially only covalent FAD (>95%), obtained as described under "Experimental Procedures." The absence of substantial quantities of the apoprotein form was assessed based on the $A_{278\ nm}/A_{450\ nm}$ ratio that was ≤14.5.

In a general context spectral effects in flavoproteins reflect modifications of the microenvironment at the active site. The spectra of recombinant and commercial wild-type BCOs are identical. This provides a basis for comparison with previous studies done with the latter (12). In general, mutations induce a minor hypochromic effect on the main absorption band in the visible (Fig. 2). This is depicted for the Glu-311 mutants in Fig. 2*A*, where also a 7–10-nm shift of its maximum to longer wavelengths is evident. In the case of Arg-477 mutants, and particularly of R477A BCO, the spectral shape (Fig. 2*B*) is modified to reflect a more hydrophobic environment (26). Minor alterations of the absorption spectrum were also observed for the other BCO mutants (Figs. 2, *C* and *D*, and Table 1); this is consistent with the assumption that the modifications at the active center induce only minor structural effects. Noteworthy, the near- and far-UV CD spectra of all BCO mutants (not shown) are similar to that of wild-type BCO, thus confirming the absence of main conformational changes.

The reduced forms of BCOs were obtained by anaerobic reduction with cholesterol. Wild-type BCO and the A204C, G309C, E311D/Q, E475D/Q, and R477K BCO mutants are completely reduced within a few seconds by a 2–5 molar excess of cholesterol. G309A and I423L/I423V mutants were also promptly reduced but only after the addition of about a 20-fold molar excess of cholesterol. The obtained spectra are characteristic of reduced flavoproteins, with minor differences for individual mutants (not shown), again suggesting the absence of major differences in the interactions of reduced flavin and environment. On the other hand, for the E311L BCO mutant only an ~50% flavin reduction (estimated by comparison with the fully reduced form of the E311D/Q BCO mutants) was observed using an excess up to 270-fold of cholesterol and after several hours of anaerobic incubation (Table 1). The same extent of flavin reduction (~50%) was observed with the R477A

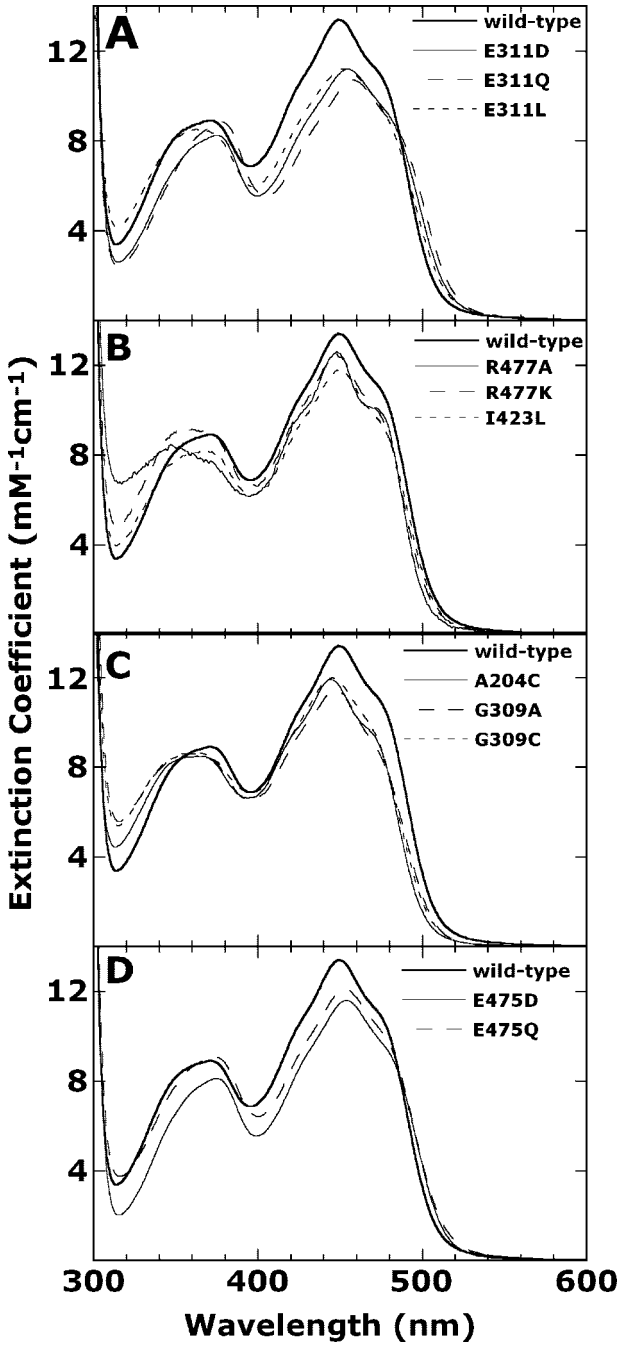

FIGURE 2. **Absorption spectra of recombinant wild-type BCO and of selected mutants.** The spectra are of the oxidized state of the enzymes, and for comparison, the trace of wild-type BCO is shown in all panels. The concentrations of the enzymes were 10–12 μM in 100 mM potassium phosphate buffer, pH 7.5, and at 15 °C; the spectra were normalized to reflect their extinction coefficients.

BCO mutant after incubation for 1 week under anaerobic conditions. Noteworthy, these latter two mutants show negligible activity in both the dehydrogenation and the isomerization reactions (see below).

Anaerobic photoreduction of wild-type and E311D/Q and E475D/Q COs leads to the formation of the kinetically stabilized, red anion semiquinone form as previously observed for commercial BCO (12). This is the species predicted for the flavin dehydrogenase/oxidase family members (27). The amount of semiquinone produced by recombinant wild-type BCO is similar to that observed with the commercial BCO (13) (Table 1). A similar extent of flavin photoreduction is also observed for the R477K BCO. However, in this case a weak, long-wavelength absorption band extending up to 600 nm was observed, and this effect was much more pronounced with R477A BCO. This is consistent with formation of the flavin neutral blue semiquinone and suggests a p*K* increase of the radical species, which can be attributed to the differences in charge and that affects the stabilization of the negatively charged anionic semiquinone (see also "Discussion" and Table 1).

Reaction with Sulfite—The ability to bind sulfite to form covalent N(5) adducts is a characteristic of flavoprotein oxidases, and it yields information on the redox potential of a given enzyme (27). This approach was used in the present work to provide criteria for a differentiation of effects resulting from alterations of redox potentials as opposed to steric factors; pertinent data are listed in Table 2. The reaction of commercial wild-type BCO with sulfite was previously found to be a second-order process (12). With the E311Q/L and E475Q BCO mutants, attainment of equilibrium is sufficiently rapid to allow an estimation of the K_d value based on results of titrations with sulfite. In all other cases the rate constant for the step of sulfite binding (k_{on}) was obtained from the slope of linear plot of the rates of adduct formation at different sulfite concentrations estimated from the decrease in absorbance at ~450 nm. For the determination of the rate of dissociation (k_{off}), the adduct was purified from excess sulfite by rapid gel-permeation chromatography, and its decay was followed by the absorbance increase at ~450 nm corresponding to the formation of oxidized enzyme. The most significant effect on the K_d values (Table 2) was observed for the removal of the positive charge at position 477.

Redox Potentials—These parameters were estimated for wild type (as a reference) and for selected BCO mutants deemed to be relevant in the present context, *i.e.* for the cases where modification of charges are expected. The data are listed in Table 2. The redox potential of recombinant BCO was measured using indigo tetrasulfonate and cresyl violet. The midpoint potential (E_m) found was −96 mV, the same as that determined earlier using commercial BCO (12). A salient point is that the implemented mutations have comparatively small effects on E_m (Table 2). These range from an increase of the midpoint potentials by ~20 mV in the case of mutations of Glu-311 and Glu-475 to a decrease of ~40 mV for the R477K mutant (Table 2). In contrast to this, a more pronounced effect of the mutations was observed on the separation between the single one-electron transfer potentials (E_1, E_2). In those cases where mutations do not induce a change of charge, the separation of E_1 and E_2 is somewhat lower (see *e.g.* R477K and E311D BCOs). When a charge is removed (E311Q and E475Q), the separation increases substantially (Table 2).

Steady-state Kinetics—The kinetic parameters for wild-type and mutants of BCO under steady-state conditions were assessed using two complementary methods: those obtained with the classical *o*-dianisidine/peroxidase assay at 0.25 mM O_2 concentration (air saturation, 25 °C, 1% Thesit, 1% 2-propanol)

TABLE 2

Parameters of the interaction of wild-type BCO and mutants with sulfite and redox potentials of selected mutants

Sulfite complex formation experiments were carried out at 15 °C in 100 mM potassium phosphate buffer, pH 7.5, at 15 °C. The rates were determined spectroscopically by following the absorbance decrease/increase at ~450 nm corresponding to sulfite binding/dissociation. Determination of redox potentials as described under "Experimental Procedures" and using the dyes listed.

Enzyme form	k_{on}	k_{off}	K_d[a]	E_m (E_1, E_2)	Redox dye[b]
	$mM^{-1}\ min^{-1}$	min^{-1}	μM	mV	
Wild-type					
Commercial[c]	0.37	0.05	140	−101[c]	IDS, CV
Recombinant	0.33 ± 0.02	0.016 ± 0.002	48	−96 (−47, −147)	ITS, CV
A204C	0.080 ± 0.005	0.038 ± 0.005	475		
G309A	0.081 ± 0.002	0.025 ± 0.003	309		
G309C	0.078 ± 0.004	0.024 ± 0.004	308		
E311D	3.4 ± 0.2	0.022 ± 0.002	6.5	−76 (−39, −113)	ITS, IDS
E311Q	33 ± 1	0.052 ± 0.008	1.6/*17 ± 4*	−84 (−13, −157)	ITS, CV
E311L	7.4 ± 0.4	0.022 ± 0.001	3/*42 ± 10*		
I423L	0.096 ± 0.011	0.01 ± 0.001	104		
I423V	0.133 ± 0.004	0.012 ± 0.001	90		
E475D	2.21 ± 0.06	0.03 ± 0.003	14		
E475Q	Fast (>50)	0.28 ± 0.02	*16 ± 4*	−87 (−18, −155)	ITS, CV
R477A	0.0019 ± 0.0001	0.021 ± 0.001	11000		
R477K	0.044 ± 0.002	0.048 ± 0.006	1100	−138 (low separation)	IDS

[a] K_d values obtained by determination of either k_{on} and k_{off} ($K_d = k_{off}/k_{on}$) or, for E311Q/L and E475Q BCOs, estimated from static titration experiments based on end points of absorbance changes (data are in *italics*).
[b] ITS, indigo tetrasulfonate (E_m = −43.3 mV); IDS, indigo disulfonate (E_m = −124 mV); CV, cresyl violet (E_m = −176 mV).
[c] Data are from Ref. 12.

TABLE 3

Apparent steady-state kinetics parameters for reactions of wild-type BCO and mutants

The parameters for cholesterol dehydrogenation (oxidation) reaction determined at constant oxygen concentrations are apparent. Conditions: 100 mM potassium phosphate buffer, pH 7.5, 1% propan-2-ol, and 1% Thesit at 25 °C, assuming an oxygen concentration of 0.25 mM (air saturation). Measurements of the isomerization reaction were done in the same buffer containing 10% propan-2-ol, 1% Thesit, at 25 °C by following the cholest-4-en-3-one formation at 240 nm. ND, not determined.

Enzyme form	Dehydrogenation (oxidation) reaction (substrate, cholesterol)			Isomerization reaction (substrate, cholest-5-en-3-one)			Ratio $k_{cat,isomerization}/k'_{cat,dehydrogenation}$
	k'_{cat}	$K'_{m,chol}$	$k'_{cat}/K'_{m,chol}$	k_{cat}	$K_{m,chol\text{-}en}$	$k_{cat}/K_{m,chol\text{-}en}$	
	s^{-1}	mM	$mM^{-1}\ s^{-1}$	s^{-1}	mM	$mM^{-1}\ s^{-1}$	
Wild-type							
Commercial	34 ± 1	0.2 ± 0.03	170	300 ± 50	0.6 ± 0.1	500	8.8
Recombinant	54 ± 4	0.31 ± 0.02	175	410 ± 70	0.5 ± 0.1	820	7.6
A204C	25 ± 1	0.31 ± 0.02	80	350 ± 5	1.0 ± 0.1	350	14
G309A	38 ± 1	0.32 ± 0.01	120	190 ± 12	0.45 ± 0.05	420	5
G309C	37 ± 1	0.21 ± 0.02	175	270 ± 6	0.55 ± 0.03	490	7.3
E311D	9.3 ± 0.5	0.14 ± 0.03	65	15 ± 1	0.05 ± 0.01	300	1.6
E311Q	0.82 ± 0.02	0.26 ± 0.05	3.2	14 ± 2	0.3 ± 0.02	47	17
E311L	0.0014 ± 0.0001	0.32 ± 0.01	0.004	0.11 ± 0.002	1.4 ± 0.1	0.08	80
I423L	51 ± 4	0.23 ± 0.06	220	320 ± 30	0.6 ± 0.1	535	6.3
I423V	28 ± 1	0.17 ± 0.01	165	320 ± 30	0.8 ± 0.1	400	11
E475D	6.5 ± 0.2	0.05 ± 0.01	130	31 ± 1	0.04 ± 0.01	775	4.8
E475Q	25 ± 6	0.10 ± 0.04	250	52 ± 1	0.17 ± 0.04	305	2.1
R477A	<0.001	ND	ND	0.6 ± 0.02	0.013 ± 0.001	45	>600
R477K[a]	1.3 ± 0.4	0.67 ± 0.20	1.9	69 ± 0.5	0.45 ± 0.02	155	53

[a] Average from Michaelis-Menten and double reciprocal plots.

and saturating cholesterol concentrations that are defined as "apparent" and indicated with quotation marks and the data obtained with the EMTN method (initial O_2 concentration = 0.125 or 0.25 mM, 25 °C) (24) that are calculated for both saturating O_2 and cholesterol concentrations. Mutations at position 204, 309, and 423 have a minor effect (≤3-fold) on k'_{cat} and K'_m for O_2-dependent turnover and for the isomerization reaction of BCO (Table 3). Most significant effects are instead observed for the Glu-475 BCO mutants (Table 3); however, because a decrease in k'_{cat} is accompanied in all cases by a decrease in K'_m, these changes do not modify (≤2-fold) the apparent k'_{cat}/K'_m ratio. A large effect was instead observed for substitution of residues Glu-311 and Arg-477. In particular, the dehydrogenation reaction decreases about 70-fold when the negative charge at position 311 is removed (E311Q), a change that also affects k_{cat} of the isomerization reaction (Table 3). The most drastic effect is observed with E311L and R477A BCOs for which both oxidation and isomerization activities are substantially lowered (Table 3). As indicated by the ratio of the corresponding k_{cat} values (last column of Table 3), the mutations have different effects on the isomerization and dehydrogenation reactions; this was particularly prominent in the cases of Arg-477, where even the most conservative modification (R477K) most significantly affected the oxidative reaction. In this context is should be reiterated that for all BCO variants tested, the isomerization reaction was not rate-limiting (Table 3).

The kinetic mechanism of the reaction of commercial wild-type BCO with cholesterol as substrate was previously investigated by a combination of steady-state and pre-steady-state measurements; it is consistent with a ping-pong mechanism (4) (Scheme 2). Steady-state measurements based on the EMTN method (see "Experimental Procedures") have been performed for recombinant wild-type and mutants of BCO that showed the most significant changes in the previous kinetic measurements (Fig. 3). It should be recalled that in this type of experi-

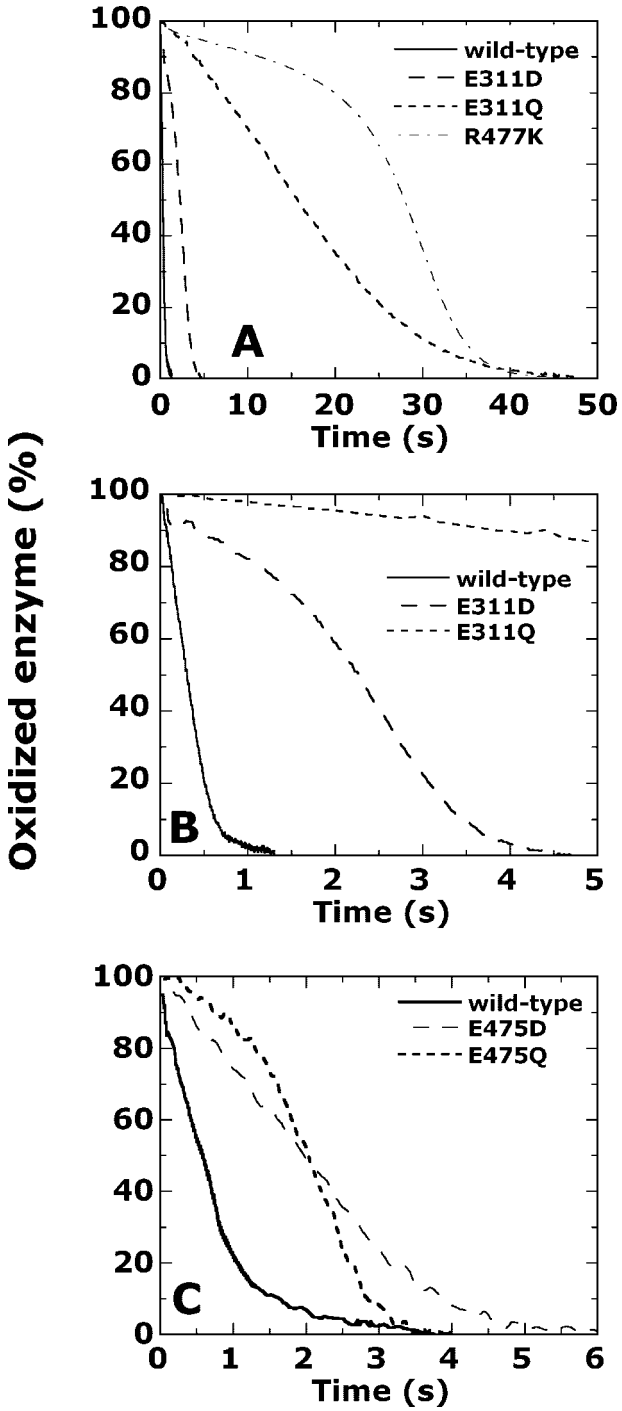

FIGURE 3. **Enzyme-monitored turnover experiments according to the method of Gibson *et al.* (24).** Wild-type and mutant BCOs (20–25 μM) in 100 mM potassium phosphate buffer, pH 7.5, 1% propan-2-ol, and 1% Thesit at 25 °C were reacted in the stopped-flow instrument with 1 mM cholesterol and 125 μM oxygen (*panels A* and *B*) or 1 mM cholesterol and 250 μM oxygen (*panel C*) (all final concentrations). The time course of the reaction was monitored at ~450 nm, and from the extinction coefficients of the oxidized *versus* reduced species (determined in separate experiments) the percentage of oxidized enzyme was normalized on the *ordinate*.

ment (24) the percentage of oxidized enzyme specie is depicted as a function of time where the area "below the experimental trace" reflects the quantity of O_2 present in the system. From this it is evident that the activity (inversely proportional to the time required for depletion of the oxygen present in the system)

TABLE 4

Steady-state kinetics parameters for the dehydrogenation (oxidation) reaction of recombinant wild-type and mutants of BCO at infinite oxygen and cholesterol concentration (EMTN method)

Measurements were in 100 mM potassium phosphate buffer, pH 7.5, 1% propan-2-ol, and 1% Thesit at 25 °C.

Enzyme form	$\Phi_0^{-1} = k_{cat}$	Φ_S	Φ_{O2}	K_m, cholesterol	K_m, O_2
	s^{-1}	μM s	μM s	mM	mM
Wild-type					
Commercial[a]	19.2	10.9	7.3	0.21	0.14
Recombinant	52 ± 4	5.8	4.2	0.3 ± 0.1	0.22 ± 0.02
E311D	10 ± 1	90	6	0.9 ± 0.1	0.06 ± 0.01
E311Q	1.1 ± 0.1	640	64	0.7 ± 0.1	0.07 ± 0.01
E475D	21 ± 3	52	9.5	1.1 ± 0.1	0.20 ± 0.03
E475Q	29 ± 6	38	3.1	1.1 ± 0.2	0.09 ± 0.01
R477K[b]	1.4 ± 0.3	1470	14	2.1 ± 0.04	0.02 ± 0.001

[a] Data from Ref. 4.
[b] Average from Michaelis-Menten and double reciprocal plots.

is significantly decreased for all mutants, the largest effect occurring with E311Q and R477K BCOs. Lineweaver-Burk plots (*i.e.* the plot reporting $1/k_{cat,app}$ *versus* $1/[O_2]$) of the kinetic data obtained according to Gibson *et al.* (24) yields parallel lines for all BCO mutants (not shown), consistent with a ping-pong mechanism as found with commercial wild-type BCO (4). The largest decrease in k_{cat} values were still observed for mutants at positions Glu-311 and Arg-477, especially when the charge was removed (Table 4). K_m values for cholesterol were higher for all mutants compared with wild-type BCO. In contrast, the K_{m,O_2} value for all BCO mutants tested was lower than for wild-type BCO and was affected significantly in the R477K mutant (Table 4). Comparison of the data in Tables 3 and 4 evidences a good correspondence between the apparent kinetic parameters (k') and those determined at infinite oxygen and cholesterol concentrations. The only exception is E475D BCO where a 3-fold difference is encountered. Differences of this parameter up to 4-fold were reported earlier for COs from varying sources (12) depending on the type of assay used. This was assumed to result from different susceptibilities of the various enzyme forms from the assay conditions (12).

Reaction of Reduced Cholesterol Oxidases with Dioxygen—The oxidation of reduced commercial wild-type BCO by O_2 can be represented by a combination of steps (Scheme 2). As discussed earlier, free reduced enzyme species are assumed to interconvert via step k_{conv}/k_{-conv} yielding a form that can react with O_2 via k_4 to yield oxidized enzyme and H_2O_2 (4). The oxidative half-reaction of position 423 mutants was not investigated in detail as their kinetic properties closely resemble those of wild-type BCO (see Table 3). Those of E311L and R477A mutants could not be studied due to their low activity and because of difficulties in obtaining the reduced forms (see Tables 1 and 3). Primary traces from stopped-flow experiments obtained by mixing the reduced enzyme with buffer solutions at varying O_2 concentrations (increase in absorbance at 455 nm *versus* time, Fig. 4) are best fitted by a biphasic (two-exponential) model in the case of wild-type, A204C, A309A/C, E311D, and E475D/Q BCOs. On the other hand, traces for E311Q and R477K mutants are best fitted using monophasic algorithms. Where a biphasic model is used, the second, slower phase accounts for maximally 5–10% of the total absorbance changes; this extent was found to depend also on the enzyme preparation

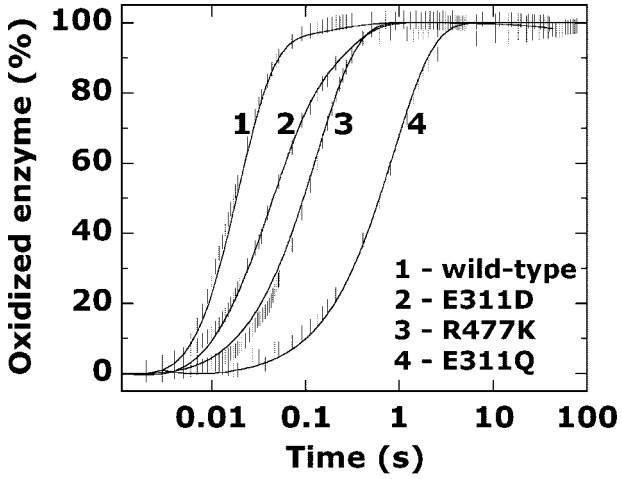

FIGURE 4. **Time course of the reaction of reduced wild-type BCO and mutants with dioxygen.** Enzymes (~12 μM) in 100 mM potassium phosphate buffer, pH 7.5, 1% propan-2-ol, and 1% Thesit at 25 °C were reduced by a 3–5 molar excess of cholesterol and were then reacted in the stopped-flow instrument with 125 μM oxygen in the same buffer. The reaction was monitored as described under "Experimental Procedures." The time courses (data points, |) are obtained from diode array spectra extracting the time dependence of the absorbance values at specific wavelengths, *e.g.* at ~450 nm. The scale of the *ordinate* is defined as in the legend to Fig. 3. The lines through the data points are fits obtained using monoexponential (*curves 3 and 4*) or biexponential algorithms (*curves 1* and *2*).

used. The corresponding rate does not depend on oxygen concentration and has values around 5 s^{-1} in all cases. This phase was not used for kinetic considerations, also since its nature is still unclear and might be related to some heterogeneity in the protein. As shown in Fig. 4, the time required to oxidize the reduced enzyme(s) varies depending on the specific mutation; it is significantly longer for E311Q and R477K BCO. The presence of superoxide dismutase (SOD, 20 units/ml) has no effect on the rate of flavin reoxidation of both wild-type and E311Q BCOs (species with a fast and a very slow rate, respectively). This is in keeping with the absence of basic changes in the mechanism of reoxidation of BCO by dioxygen induced by the mutations.

As reported earlier (4, 28), the observed rates for the main phase of oxidation (k_{obs}) of reduced wild-type BCO shows a hyperbolic saturation with increasing O_2 concentration. A similar behavior is also observed for recombinant wild-type BCO as depicted in Fig. 5*A*. This behavior has been proposed to result from the presence of a kinetic situation as represented in Scheme 2, steps k_{conv}/k_{-conv} and k_4 (4). This leads to Equation 1,

$$k_{obs} = (k_{conv} \cdot k_4 \cdot [O_2])/(k_{-conv} + k_4 \cdot [O_2]) \qquad \text{(Eq. 1)}$$

according to which the apparent rate increases with the substrate concentration until saturation is reached (28, 29).

As shown in Table 4, the k_{conv} values are substantially unmodified (≤2-fold) with A204C, G309A/C, and E475Q BCO mutants, whereas a most significant decrease is evident for E475D and R477K BCOs (see Fig. 5*B* for the latter). On the other hand, the k_4/k_{-conv} ratio was affected by these substitutions to a lesser extent. Most importantly, k_{obs} values determined for both E311D/Q BCOs show a linear dependence on O_2 concentration (Fig. 5, *A* and *B*, respectively), compatible

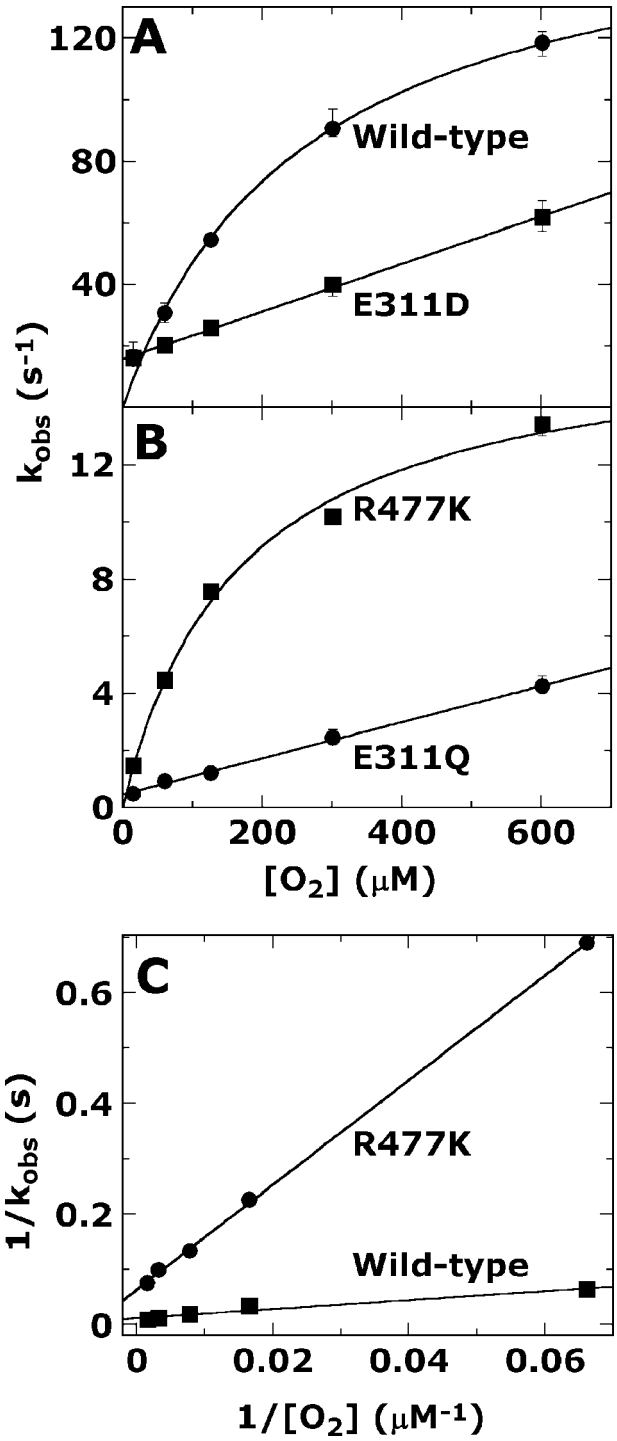

FIGURE 5. **Dependence of k_{obs}, the rate constants estimated for the reaction of reduced enzymes with dioxygen from the concentration of the latter.** The data points for rate constants were obtained as described under "Experimental Procedures" and in Fig. 4 and are the average of 5–6 single experiments. *Panels A* and *B*, the curves for wild-type and E475K BCOs are from fits based on Equation 1. The *straight lines* through the data points (E311D and E311Q BCO mutants) are from linear fits. *Panel C*, double reciprocal plot of the data for wild-type and R477K BCO; the fit through the data points is based on the reciprocal of the equation above. The values of k_{conv} (1/*y* intercept) and k_4/k_{-conv} (*x* intercept) have been estimated from such plots (see text). Where error bars are not visible the data scatter is smaller than the size of the symbols.

with a second order reaction (pseudo-first order process) (29). This behavior would result when the preceding interconversion (Scheme 2) was absent or much faster than oxidation. Interest-

TABLE 5

Rate constants for the reaction of reduced wild-type BCO and mutants with dioxygen

Measurements were in 100 mM potassium phosphate buffer, pH 7.5, 1% propan-2-ol, and 1% Thesit (final concentrations in the cuvette) at 25 °C and as detailed in the text. k_4 was obtained from experiments such as in Fig. 4 and subsequent double reciprocal plots as in Fig. 5*C*. According to Refs. 14, 28, and 29, in the double reciprocal plot ($1/k_{obs}$ *vs.* $1/O_2$ concentration), the *y* axis intercept yields $1/k_{conv}$ whereas the *x* axis intercept corresponds to k_4/k_{-conv}. For examples of "saturation" *vs.* "linear" behavior, see Fig. 5. k_{conv} and k_{-conv} refer to assumed conversions between two reduced enzyme forms before the oxygen reaction, as outlined in Scheme 2. ND, not determined. $k_4 = 1/\Phi_{O2}$ is derived from EMTN experiments (Table 4) as detailed (4).

Enzyme form	Pattern of k_{obs} *vs* $[O_2]$ plot	k_{conv}	k_4/k_{-conv} (=$1/K_d$)	k_4	
				From secondary plots	(= $1/\Phi_{O2}$) from EMTN data ($k_{cat}/K_{m,O_2}$)
		s^{-1}	mM^{-1}	$mM^{-1}s^{-1}$	
Wild type					
Commercial[a]	Saturation	170 ± 30	4.8		140
Recombinant	Saturation	240 ± 70	2.3		240
A204C	Saturation	270 ± 40	1.5		ND
G309A	Saturation	200 ± 35	4.3		ND
G309C	Saturation	110 ± 19	5.2		ND
E311D	Linear			71 ± 6	170
E311Q	Linear			6.3 ± 0.2	16
E475D	Saturation	63 ± 7	3.5		105
E475Q	Saturation	130 ± 15	5.1		325
R477K	Saturation	15.3 ± 1.4	6.9		70

[a] Data are from Ref. 4.

ingly, the elimination of a negative charge at position 311 (E311Q BCO mutant) led to an ~10-fold slower oxidation rate constant k_4 compared with wild-type BCO (Table 5, Fig. 5).

DISCUSSION

A major purpose of the present work is a comparison of the reactivity of wild-type BCO with dioxygen with that of various mutants with the substitutions of amino acid residues mentioned in the Introduction. A precondition for this is that mutations do not alter significantly (other) basic properties of the enzymes to be compared. Based on inspection of general spectral properties and specifically of the CD spectra (not shown), it appears that the introduced amino acid substitutions do not affect the folding pattern of BCO. On the other hand and in the context of the process of folding, an unexpected observation was stumbled upon; there is a dependence of the extent of formation of the covalent linkage between His-121 and the flavin (flavinylation) from mutations that are at substantial distance (up to 21 Å in the case of the residue Gly-309) from the point of linkage itself (C8α atom of FAD). This suggests that a variety of distant mutations can affect the local conformations necessary for flavinylation. This topic, although of general interest (30), will not be addressed here and will be the subject of future studies. A drawback resulting from the mentioned heterogeneity of flavinylation is that it leads to the production of mixtures of purified protein forms (flavinylated and non-flavinylated), the reactivity of which differ substantially (13). Of basic importance for the present study was, thus, the ability to generate BCO proteins that are close to homogeneity with respect to flavinylation. A ≥95% purity was achieved by selective denaturation and exploiting the higher thermolability of not flavinylated BCOs (Table 1).

The effects induced by mutagenesis on the spectra of the oxidized proteins, on the formation/stability of the anionic (red) or neutral (blue) semiquinone forms, on the stability of the sulfite adducts, and on the redox potentials (Table 1 and 2) is taken as to reflect the modification of charges and of dielectric properties. Obviously these could also be factors to consider in comparing rates of oxygen reactivity (see below). It should be recalled that the redox potential of the flavin cofactor is affected not only by charges/dipoles in its immediate vicinity but also by the "global charge" in its further environment as demonstrated by Swenson and Zhou (31, 32) for flavodoxins. The data listed in Table 2 for sulfite binding to BCO mutants show that mutations lead maximally to an ~10-fold increase and an ≈20-fold decrease in K_d, with the exception of R477A where the elimination of a neutralizing charge probably has an important effect. In agreement with this, the effects of mutations on the redox potentials of BCO are rather small and within 40 mV of the E_m value for wild-type BCO (Table 2).

Inspection of Table 3 reveals that the E311L and R477A mutations have substantial effects on the kinetic parameters for turnover with cholesterol as substrate and on the isomerization reaction. This is taken as suggesting that in these specific cases the catalytic machinery is disrupted, possibly for steric (E311L) and charge balance (R477A) reasons. Interestingly, the K_m for cholesterol is affected to a lesser extent. The finding of considerable activity with E311Q indicates that the carboxylate of Glu-311 is not essential for catalysis but probably assists in the correct positioning of Arg-477. This is in contrast with the conclusions inferred from comparison of the three-dimensional structure of covalent and non-covalent COs (1, 15). A positive charge at position 477, however, appears to be crucial since its removal lowers activity by ~5 orders of magnitude. This effect is likely to be the combination of several factors, the one on the redox potential, as reflected by a 100-fold higher K_d for formation of the sulfite adduct probably being important (Table 2).

In general, the mutations introduced in BCO affect the k_{cat} for substrate dehydrogenation more than the rate of isomerization. Instead, with the Glu-475 mutants the opposite is observed (lower $k_{cat,isomerization}/k'_{cat,dehydrogenation}$, Table 3). The isomerization of cholest-5-en-3-one to the 4-en-3-one has been proposed by Coulombe *et al.* (15) to be catalyzed by Glu-475. Because the isomerization activity is lowered only ~7-fold for the E475Q mutant, it is unlikely that Glu-475 is an essential residue intimately involved in this step. On the other hand, from the data listed in Table 3 it is apparent that Glu-311 plays

a predominant role as its mutation has an ~1000-fold effect on dehydrogenation activity. A supportive role of, or a combination with Arg-477 is probable. The latter is within H-bonding distance from the steroid OH-group and forms a H-bond to the carboxylic group of Glu-311 in the gate open conformation (15).

Turning to the oxygen reactivity of reduced wild-type and mutants of BCO (Table 5), it appears that in the cases where a saturation behavior of k_{obs} *versus* O_2 concentration occurs, the observed rates are significantly altered only for R477K BCO (see Fig. 5). On the other hand, the data in Fig. 5 and Table 5 also highlight the most prominent result of the present study, namely the finding that mutation of Glu-311 leads to a basic change in the mechanism by which O_2 reacts with reduced BCO. Thus, removal of Glu-311 converts the "saturation behavior" of the rate of reoxidation *versus* O_2 concentration to a linear dependence that might reflect an apparent second order reaction. Saturation behavior is specific of this oxidase and is assumed to result from an equilibrium between two reduced enzyme forms where one preferentially reacts with oxygen (4, 28). A linear dependence is common of most flavoproteins oxidases and reflects an apparent second order reaction (29). It should be emphasized that the effects on the rates of oxygen reactivity of the Glu-311 mutants are most likely not attributable to alterations of the redox potentials since the minor modification (Table 2) cannot account for the observed effects. This also agrees with the observation that a reduction of the rates of oxygen reactivity is induced by the E311Q and the R477K mutations, whereas the corresponding E_m values move in opposite directions (Table 2). The present interpretations are in keeping with the earlier assumption (4, 23) that the kinetic behavior of BCO with O_2 is not due to "artifacts" resulting *e.g.* from the presence of micelles in the system. To the contrary, it lends support to the mechanism that emerged from the three-dimensional structure of BCO (15) in which the pair Glu-475—Arg-477 was found in different conformations named gate open/gate closed as shown in Fig. 1. That the switch from saturation behavior (possibly related to an interconversion situation such as depicted in Scheme 2) to an apparent bimolecular mechanism (Fig. 5) occurs with the mutation of Glu-311 is somewhat surprising. It suggests that the Glu-475—Arg-477 gate is finely tuned by Glu-311 and that an additional separation by 2–3 Å (the equivalent of a -CH_2 segment) of the -COO^- charge from the positive one of Arg-477 is sufficient to alter the mode of interaction. Interestingly, the longer chain of lysine present in R477K BCO mutant does not appear to disrupt the interaction, although the k_{conv} rate constant appears to be reduced, this resulting in a lower reactivity with oxygen. These effects are compatible with the decrease of the rate of interconversion of the reduced enzyme forms (closed form *versus* open form, see Scheme 2), although other mechanisms cannot be excluded.

A hypothesis concerning the role and function of the discussed channel and gate can be formulated; a saturation mechanism might serve in a better utilization of oxygen at low concentrations (sequestration), whereas the gating could be involved in regulating the reactivity of the reduced enzyme-product complex. The present results should be viewed also in the context of recent studies dealing with the mode of access/diffusion of O_2 in various proteins containing a heme moiety. In several cases specific channels have been identified, and the kinetics of the diffusion process has been studied (16–20). It, thus, appears that the presence of specific channels that might be regulated is a common theme in enzymes that act on dioxygen.

REFERENCES

1. Lario, P. I., Sampson, N., and Vrielink, A. (2003) *J. Mol. Biol.* **326,** 1635–1650
2. MacLachlan, J., Wotherspoon, A. T., Ansell, R. O., and Brooks, C. J. (2000) *J. Steroid Biochem. Mol. Biol.* **72,** 169–195
3. Sampson, N. S. (2001) *Antioxid. Redox Signal.* **3,** 839–846
4. Pollegioni, L., Wels, G., Pilone, M. S., and Ghisla, S. (1999) *Eur. J. Biochem.* **264,** 140–151
5. Purcell, J. P., Greenplate, J. T., Jennings, M. G., Ryerse, J. S., Pershing, J. C., Sims, S. R., Prinsen, M. J., Corbin, D. R., Tran, M., Sammons, R. D., and Stonard, R. J. (1993) *Biochem. Biophys. Res. Commun.* **196,** 1406–1413
6. Corbin, D. R., Grebenok, R. J., Ohnmeiss, T. E., Greenplate, J. T., and Purcell, J. P. (2001) *Plant Physiol.* **126,** 1116–1128
7. Machang'u, R. S., and Prescott, J. F. (1991) *Can. J. Vet. Res.* **55,** 332–340
8. Fuhrmann, H., Dobeleit, G., Bellair, S., and Guck, T. (2002) *J. Vet. Med. B Infect. Dis. Vet. Public Health* **49,** 310–311
9. Pei, Y., Dupont, C., Sydor, T., Haas, A., and Prescott, J. F. (2006) *Vet. Microbiol.* **118,** 240–246
10. Ladron, N., Fernandez, M., Agüero, J., Gonzales Zörn, B., Vasquez-Boland, J. A., and Navas, J. (2003) *J. Clin. Microbiol.* **41,** 3241–3245
11. Vrielink, A., Lloyd, L. F., and Blow, D. M. (1991) *J. Mol. Biol.* **219,** 533–554
12. Gadda, G., Wels, G., Pollegioni, L., Zucchelli, S., Ambrosius, D., Pilone, M. S., and Ghisla, S. (1997) *Eur. J. Biochem.* **250,** 369–376
13. Motteran, L., Pilone, M. S., Molla, G., Ghisla, S., and Pollegioni, L. (2001) *J. Biol. Chem.* **276,** 18024–18030
14. Li, J., Vrielink, A., Brick, P., and Blow, D. M. (1993) *Biochemistry* **32,** 11507–11515
15. Coulombe, R., Yue, K. Q., Ghisla, S., and Vrielink, A. (2001) *J. Biol. Chem.* **276,** 30435–30441
16. Hofacker, I., and Schulten, K. (1998) *Proteins Struct. Funct. Genet.* **30,** 100–107
17. Soulimane, T., Buse, G., Bourenkov, G. P., Bartunik, H. D., Huber, R., and Than, M. E. (2000) *EMBO J.* **19,** 1766–1776
18. Brunori, M. (2000) *Biophys. Chem.* **86,** 221–230
19. Draghi, F., Miele, A. E., Travaglini-Allocatelli, C., Vallone, B., Brunori, M., Gibson, Q. H., and Olson, J. S. (2002) *J. Biol. Chem.* **277,** 7509–7519
20. Deng, P., Nienhaus, K., Palladino, P., Olson, J. S., Blouin, G., Moens, L., Dewilde, S., Geuens, E., and Nienhaus, G. U. (2007) *Gene* (*Amst.*) **398,** 208–223
21. Sambrook, J., Fritsch, E. F., and Maniatis, T. (1989) *Molecular Cloning: A Laboratory Manual*, 2nd Ed., Cold Spring Harbor Laboratory, Cold Spring Harbor, NY
22. Whitby, L. G. (1954) *Biochim. Biophys. Acta* **15,** 148–149
23. Lim, L., Molla, G., Guinn, N., Ghisla, S., Pollegioni, L., and Vrielink, A. (2006) *Biochem. J.* **400,** 13–22
24. Gibson, Q. H., Swoboda, B. E., and Massey, V. (1964) *J. Biol. Chem.* **239,** 3927–3934
25. Massey, V., and Hemmerich, P. (1978) *Biochemistry* **17,** 9–16
26. Muller, F., Mayhew, S. G., and Massey, V. (1973) *Biochemistry* **12,** 4654–4662
27. Massey, V., and Hemmerich, P. (1980) *Biochem. Soc. Trans.* **8,** 246–257
28. Schopfer, L. M., Massey, V., Ghisla, S., and Thorpe, C. (1988) *Biochemistry* **27,** 6599–6611
29. Strickland, S., Palmer, G., and Massey, V. (1975) *J. Biol. Chem.* **250,** 4048–4052
30. Edmondson, D. E., and Newton-Vinson, P. (2001) *Antioxid. Redox Signal.* **3,** 789–806
31. Zhou, Z., and Swenson, R. P. (1995) *Biochemistry* **34,** 3183–3192
32. Zhou, Z., and Swenson, R. P. (1996) *Biochemistry* **35,** 15980–15988